PERGAMON

International Journal of Heat and Mass Transfer 41 (1998) 4081–4093

International Journal of HEAT and MASS TRANSFER

Temperature fluctuations in particle-laden homogeneous turbulent flows

F. A. Jaberi*

Department of Mechanical and Aerospace Engineering, State University of New York at Buffalo, Buffalo, NY 14260, U.S.A.

Received 12 September 1997; in final form 9 April 1998

Abstract

The statistical behavior of the fluid and particle temperatures in homogeneous two-phase turbulent flows are investigated via direct numerical simulations. The effects of the flow Reynolds number (Re_λ), the Prandtl number (Pr), the particle response time (τ_p), the ratio of specific heats (α), and the mass loading ratio (ϕ_m) on the fluid and particle temperature statistics are studied. The results show that the particle temperature intensity decreases as the magnitudes of τ_p, Pr, α, and Re_λ increase. Also, by decreasing the magnitudes of α and/or Pr, the difference between the particle velocity and temperature diffusivity coefficients increases. The ratio of particle to fluid temperature intensities and the dissipation rate of the fluid temperature are affected by two-way coupling effects and decrease as the mass loading ratio increases. Additionally, with increased mass loading, the probability density function of the fluid temperature deviate more from the Gaussian distribution.

Nomenclature

C_D drag coefficient
D_u^f diffusion coefficient of the fluid particle velocity
D_T^f diffusion coefficient of the fluid particle temperature
D_v^p diffusion coefficient of the particle velocity
D_T^p diffusion coefficient of the particle temperature
d_p particle diameter
F_i velocity forcing function
k magnitude of the Fourier wave number
m_p particle mass
Nu Nusselt number
N_p total number of particles
Pr Prandtl number
p pressure
R_u^f auto-correlation coefficient of the fluid particle velocity
R_v^p auto-correlation coefficient of the particle velocity
R_T^p auto-correlation coefficient of the particle temperature
Re_0 reference Reynolds number
Re_p particle Reynolds number
Re_λ Taylor micro-scale Reynolds number
St Stokes number
S_H heat source term
S_{Mi} ith component of the momentum source term
t time
T fluid temperature
T_p particle temperature
u_i ith component of the fluid velocity **U**
v_i ith component of the particle velocity **V**
X_i Lagrangian coordinates
x_i Eulerian coordinates.

Greek symbols

α ratio of the specific heat of the particle to that of the fluid
ε dissipation rate of turbulent kinetic energy
ε_p rate of energy transfer by particle drag force
ε_T dissipation rate of the fluid temperature
η Kolmogorov length scale
Θ temperature forcing function
ξ_T correlation coefficient between temperature and its dissipation rate
ρ fluid density
ρ_p particle density
τ_k Kolmogorov time scale
τ_l Eulerian integral time scale

* Corresponding author. Tel.: +001-716-645-2593; Fax: +001-716-645-3875; E-mail: jaberi@eng.buffalo.edu

0017–9310/98 $19.00
PII: S0017–9310(98)00162–8

τ_p particle response time
ϕ_m mass loading ratio.

1. Introduction

Within the past few decades, particle-laden turbulent flows have been extensively studied via theoretical, experimental and numerical methods (for the latest reviews see Refs [1–6]). Most of the theoretical studies are based on the Lagrangian statistical approach. Lagrangian analysis of turbulent flows dates back to Taylor [7] who relates fluid particle dispersion to the Lagrangian auto-correlation of fluid elements. Since then, Taylor's theory has been the basis of many other theoretical investigations involving the dispersion of fluid and light tracer particles [8–10]. Contrary to light tracer particles, heavy particles do not follow turbulent fluctuations of the carrier fluid, making their statistical analysis more complex. Theoretical studies of heavy particle motion have been mainly focused on the effects of the turbulence, the particle inertia, and the gravitational drift on the dispersion of particles [11–15].

The statistical behavior of heavy particles has also been studied via numerical methods [16]. In these studies, the velocity of the fluid surrounding the particle is often calculated based on the turbulence models for the fluctuating velocity. Assessments of such models are difficult due to the lack of sufficient experimental data. The experimental studies of particle-laden turbulent flows are somewhat limited (e.g., [17–19]) primarily due to the difficulties in Lagrangian measurements.

Some of the constraints involved in the numerical analysis of particle laden turbulent flows are avoided in direct numerical simulations (DNS) in which all scales of the fluid motion are resolved [20]. Riley and Patterson [21] were the first to present a full simulation of small particle motion in a decaying isotropic flow field. Their simulation shows that in the absence of gravity, the Lagrangian auto-correlation of the particle velocity increases as the response time (inertia) of the particles increases. The dispersion of heavy particles in forced and decaying isotropic turbulence is studied by Squires and Eaton [22] and Elghobashi and Truesdell [23]. In agreement with the theoretical findings [13, 24], their results indicate that in both decaying and forced turbulence the dispersion of the heavy particles is greater than that of the fluid particles. The effect of heavy particles on the carrier fluid in forced turbulence was studied by Squires and Eaton [25] via DNS. The results of this study indicate that the particle field attenuates an increasing fraction of the turbulence kinetic energy as the mass loading ratio increases.

None of the studies mentioned above consider the heat transfer between the particles and the carrier fluid. The behavior of the particle and carrier fluid temperatures in two-phase turbulent flows is of intense practical importance. For example, evaporation and combustion of particles in industrial devices, as well as the dispersion of thermal pollutants in the atmosphere and ocean depend strongly on the thermal transport between the phases. There are only a few investigations which study the temperature variations in two-phase turbulent flows. Soo [26] and Shraiber et al. [27] consider some of the statistical properties of the particle temperature. Using a theoretical model, Yarin and Hetsroni [28] show that an increase in the particle mass loading ratio and particle specific heat leads to a reduction in the intensity of the particles and carrier fluid temperatures. They also show that the fluctuations of the carrier fluid temperature increase and those of the particles' temperature decrease as the magnitude of the Prandtl number increases. The dynamics of evaporating particles in a heated jet is studied numerically by Park et al. [29]. The results of this investigation indicate the complexities of heat and mass transfer in two-phase free-shear flows. Although the information provided in Refs [26–29] are valuable, they are not obviously sufficient. More elaborate studies are required to fully understand and to model the temperature behavior in two-phase turbulent flows.

The primary objective of this work is to study the response of the particle temperature to the variations in the fluid temperature, and to examine the effect of the particles on the fluid temperature field. The influence of various flow and particle parameters on the statistics are examined in detail. The analysis is restricted to dilute particle motions in homogeneous incompressible turbulent flows. The homogeneity assumption avoids the complexities that are involved in nonlinear mean transport of statistical quantities and can be realized in several experimental setups such as grid turbulence and the plug flow reactor. The incompressibility is a valid assumption if the intensity of temperature fluctuations is small [30, 31].

2. Governing equations and computational methodology

In this section, the governing equations are presented and the computational methodology used for solving these equations is discussed. The transport of the carrier fluid velocity and temperature are treated in the Eulerian frame of reference and are governed by the continuity, momentum and energy equations which include source terms accounting for the presence of the particle phase. These source terms represent (the momentum and the thermal) coupling between the carrier fluid and the particles. For a constant density flow, the normalized form of the fluid equations are expressed as:

$$\frac{\partial u_j}{\partial x_j} = 0 \tag{1}$$

$$\frac{\partial u_i}{\partial t} + \frac{\partial (u_i u_j)}{\partial x_j} = -\frac{\partial p}{\partial x_i} + \frac{1}{Re_0}\frac{\partial^2 u_i}{\partial x_j \partial x_j} + F_i + S_{Mi} \tag{2}$$

$$\frac{\partial T}{\partial t} + \frac{\partial (u_j T)}{\partial x_j} = \frac{1}{Re_0 Pr}\frac{\partial^2 T}{\partial x_j \partial x_j} + \Theta + S_H. \tag{3}$$

The variables F_i and Θ are the stochastic forcing functions which are introduced to maintain the stationarity of the velocity and temperature fluctuations [32]. The turbulent scales remain invariant and the statistical analysis are convenient when the flow is statistically stationary. All variables in the above equations are normalized using reference length (L_0), velocity (U_0), temperature (T_0) and density (ρ_0) scales (the non-dimensional density is unity). Consequently, the two important non-dimensional parameters are the box Reynolds number ($Re_0 = \rho_0 U_0 L_0/\mu$, μ is the fluid viscosity) and the Prandtl number (Pr). The effects of the particles on the carrier fluid are expressed through the momentum (S_{Mi}) and heat (S_H) source terms as defined below.

The main assumptions in deriving the particle equations and the associated source terms are that the particles are fine and heavy and the mixture is dilute. Under these conditions, particle collisions are infrequent and particle–particle interactions can be neglected. The transport properties of spherical particles in non-uniform flows have been the subject of numerous investigations [33–35, 6]. Starting from simple Stokes relations, complex empirical relations have been proposed. For the range of particle Reynolds numbers considered here, it is adequate to use the modified Stokes relations for the particle transport coefficients [36, 6]. Radiative heat transfer effects and particle acceleration due to forces other than the drag force are ignored. Consequently, the evolution of the particle displacement vector (X_i), the velocity vector (v_i) and the temperature (T_p) are governed by the following equations:

$$\frac{dX_i}{dt} = v_i \tag{4}$$

$$\frac{dv_i}{dt} = \frac{C_D Re_p}{24\tau_p}(u_i^* - v_i) \tag{5}$$

$$\frac{dT_p}{dt} = \frac{Nu}{3\alpha Pr \tau_p}(T^* - T_p) \tag{6}$$

where the asterisk refers to the local fluid variables which are interpolated to the particle position. The non-dimensional particle time constant (τ_p) is;

$$\tau_p = \frac{Re_0 \rho_p d_p^2}{18} = \frac{\rho_p^{1/3} Re_0}{18}\left(\frac{6m_p}{\pi}\right)^{2/3}. \tag{7}$$

The magnitude of ρ_p is 1000 unless otherwise stated. The particle drag coefficient (C_D), the Reynolds number (Re_p) and the Nusselt number (Nu) in the modified Stokes relations are expressed by [37]:

$$C_D = \frac{24(1 + 0.15 Re_p^{0.687})}{Re_p} \tag{8}$$

$$Re_p = Re_0 \rho^* d_p |\mathbf{U}^* - \mathbf{V}| \tag{9}$$

$$Nu = 2 + 0.6 Re_p^{0.5} Pr^{0.33}. \tag{10}$$

The volumetric source terms appearing in the fluid equations (S_{Mi} and S_H) are evaluated based on the discrete Particle-Source-In Cell (PSIC) model [36] and are expressed as:

$$S_{Mi} = -\frac{1}{\Delta V}\sum\left\{m_p \frac{dv_i}{dt}\right\} = -\frac{1}{\Delta V}\sum\left\{\frac{C_D Re_p m_p}{24\tau_p}(u_i^* - v_i)\right\} \tag{11}$$

$$S_H = -\frac{1}{\Delta V}\sum\left\{\alpha m_p \frac{dT_p}{dt}\right\} = -\frac{1}{\Delta V}\sum\left\{\frac{Num_p}{3Pr\tau_p}(T^* - T_p)\right\} \tag{12}$$

where the summation is taken over all particles in the volume $\Delta V = (\Delta x)^3$ (Δx is the grid spacing) centered at each Eulerian (grid) point. In the derivation of equations (3) and (12), the heat generated by the viscous dissipation of the turbulent motions as well as that due to the particle drag force are neglected.

The transport equations of the fluid mass, momentum and heat (equations (1)–(3)) are integrated using the Fourier pseudo-spectral method with triply periodic boundary conditions [38, 39]. All simulations are conducted within a box containing 96^3 collocation points. Aliasing errors are treated by truncating the Fourier values outside the shell with wavenumber $k_{max} = \sqrt{2}N/3$ (where N is the number of grid points in each direction). The explicit second order accurate Adams–Bashforth scheme is used for time advancement. The forcing scheme is similar to that of Eswaran and Pope [40] in which the spectral contents of velocity and temperature fluctuations within the wavenumber band $0 < |\mathbf{K}| \leq k_F$ ($\mathbf{K}$ is the wavenumber vector and $k_F = 2\sqrt{2}$ is the forcing radius) are kept statistically constant by randomly forcing all nodes within that band. The magnitudes of the flow Reynolds and Prandtl numbers vary for different cases but are selected such that all variables are adequately resolved. This is enforced by keeping the magnitude of ηk_{max} (η is the Kolmogorov length scale) greater than 1.4.

Once the fluid velocity and temperature fields are known, the particle momentum and heat transfer equations (equations (5)–(6)) and the particle trajectory equation (equation (4)) are integrated via the second order Adams–Bashforth scheme. The evaluation of the fluid quantities at the particle locations is based on a fourth order accurate Lagrangian interpolation scheme. The number of particles varies in different simulations but is never less than 28^3. This number of particles is sufficient

to calculate the statistics with less than 1% error. In the discussion of the results below, $\langle\langle\ \rangle\rangle$ denotes the Lagrangian average taken over ensembles of particle or fluid elements. The Eulerian average is denoted by $\langle\ \rangle$ and is conducted over all collocation points. Time averaged statistics are denoted by an overbar and are performed after a stationary condition is sustained. The 'prime' denotes the mean subtracted quantity.

3. Results

The results of our simulations indicate that the important statistical quantities such as the Lagrangian autocorrelation coefficient of particle temperature and the ratio of particle to fluid temperature intensities are insensitive to the fluid temperature intensity (or the amplitude of the temperature forcing function). Therefore, only results of those simulations in which the fluid temperature intensity is small are considered. Additionally, the mean values of the particle velocity and temperature are constant and equal to those of the carrier fluid. In stationary turbulence, the long time values of the particle and fluid statistics are independent of the initial conditions and are characterized by the fluid and particle parameters (i.e., τ_p, Pr, α, ϕ_m and Re_λ). The influence of these parameters on the statistics are studied in both one- and two-way coupling formulations. In the former, the mass loading ratio is negligible and the effects of particles on the flow are ignored. In the latter, the effects of particles on the flow are taken into account.

3.1. One-way coupling

The results of previous studies indicate that the statistics of the particle velocity are strongly dependent on the particle inertia or particle response time, τ_p. The statistical behavior of the particle temperature, in addition to τ_p, depends on α and Pr. This is indicated in equation (6) and is also illustrated in Fig. 1 where the ratio of the particle to fluid temperature intensities (root mean squares) is considered. Figure 1(a) shows that the ratio of the temperature intensities monotonically decreases as the magnitude of the particle response time increases. This is understandable since by increasing the particle response time, the ability of the particles to follow the fluctuations of the fluid velocity and temperature reduces. However, the rate at which the particle temperature intensity decreases with τ_p is lower for lower values of Pr. With decreasing the magnitude of Prandtl number (increasing the thermal diffusivity), the particle temperature becomes closer to the surrounding fluid temperature and less sensitive to the magnitude of the particle response time. The particle temperature intensity also decreases as the magnitude of α increases (Fig. 1(b)). With increasing the thermal capacity of the particles,

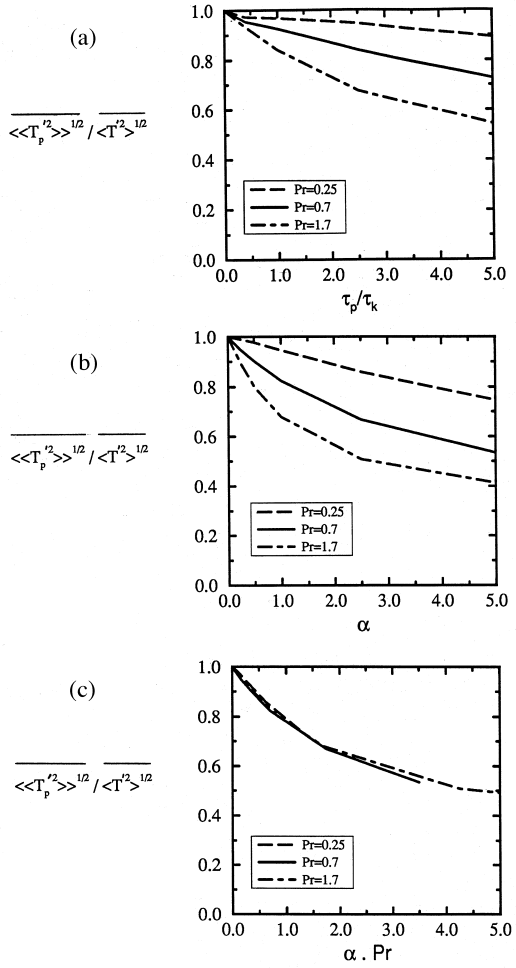

Fig. 1. The variation of the ratio of the particle to fluid temperature intensities with, (a) τ_p/τ_k and Pr ($\alpha = 1$); (b) α and Pr ($\tau_p = 3$); (c) αPr. For all cases $Re_\lambda = 41.9$.

their ability to adjust to the surrounding temperature reduces and their temperature intensity decreases. For $\alpha \ll 1$, the particle temperature intensity could be larger than the particle velocity intensity. For $\alpha \gg 1$, the fluctuations of the particle temperature are small and more sensitive to the variations in particle response time. The results in Fig. 1(a) and (b) are qualitatively consistent with the theoretical results of Yarin and Hetsroni [28] and can be further explained by considering equation (6). In accord with this equation, it is expected that by increasing τ_p, Pr and α or by decreasing Re_p (decreasing Nu), the particle temperature intensity decreases. Equation (6) also implies that for constant τ_p, particle temperature statistics are only function of the magnitude of αPr. However, the structure of the fluid temperature field, especially at the small scales, depends on the magnitude of Pr and even for a fixed value of αPr, the particle

temperature statistics could be a function of Pr. The results in Fig. 1(c) indicate that the values of $\overline{\langle\langle T_p'^2\rangle\rangle}^{1/2}/\overline{\langle T'^2\rangle}^{1/2}$ are almost independent of the magnitude of Pr. This suggests that the low order moments are not significantly dependent on the Prandtl number as long as the magnitude of αPr is kept constant.

To assess the effect of the flow Reynolds number on the particle temperature, it is necessary first to examine the variation of the particle velocity with Reynolds number. In Fig. 2(a), the ratio of the particle velocity variance (energy) to that of the carrier fluid ($\overline{\langle\langle v'^2\rangle\rangle}/\overline{\langle u'^2\rangle}$, $v'^2 = 1/3 v_i v_i$, $u'^2 = 1/3 u_i u_i$) for different τ_p and Re_λ is considered. The results in this figure indicate that the energy ratio decreases as τ_p and/or Re_λ increases. With increasing the Reynolds number, the associated time scales of the flow at large scales (i.e., Eulerian eddy turn over time) and small scales (i.e., Kolmogorov time scale) are decreased. Therefore, the 'effective' response time of the particles increase and the energy ratio decreases. It should be mentioned that the 'actual' particle response time, $\hat{\tau}_p = \tau_p/(1+0.15Re_p^{0.687})$ is different than τ_p which is considered in Figs 1 and 2. However, for the range of particle Reynolds numbers considered here, the difference between $\hat{\tau}_p$ and τ_p is small and has no significant effect on the results.

The scaling of $\overline{\langle\langle v'^2\rangle\rangle}/\overline{\langle u'^2\rangle}$ is very important in modeling of the particle-laden turbulent flows [15, 41]. An important parameter for the scaling of particle statistics

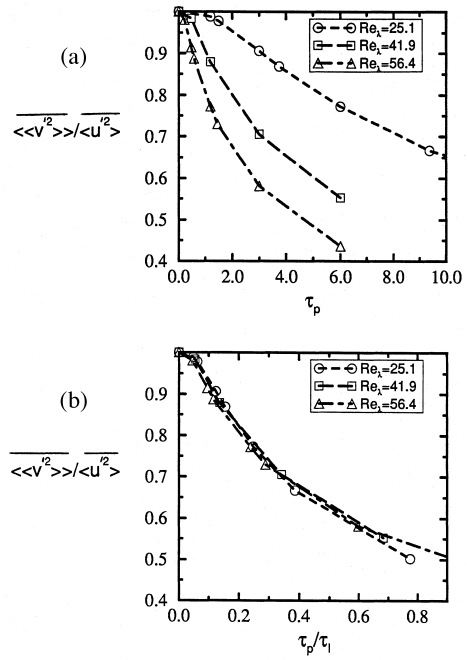

Fig. 2. The variation of the ratio of the particle to fluid velocity variances (energies), with (a) τ_p, (b) τ_p/τ_l. For all cases $\alpha = 1$ and $Pr = 0.7$.

with flow Reynolds number is the Stokes number, St [42, 43], which is the ratio of the particle response time to an 'appropriate' time scale of the turbulence. The choice of a proper flow time is, however, somewhat ambiguous. The best time scale for scaling of the low order statistics is the characteristic time associated with the large scales. This is demonstrated in Fig. 2(b), where it is shown that the values of $\overline{\langle\langle v'^2\rangle\rangle}/\overline{\langle u'^2\rangle}$ at different Re_λ collapse when the particle response time is normalized by the Eulerian eddy turn-over time, τ_l (i.e., $St_l = \tau_p/\tau_l$). Other results (not shown) also suggest that the Kolmogorov time scale (τ_k) is appropriate for scaling of $\overline{\langle\langle v'^2\rangle\rangle}/\overline{\langle u'^2\rangle}$ if the magnitude of τ_p is close or less than τ_k (i.e., $St_k = \tau_p/\tau_k < 1$). As St_k exceeds from unity, the results for $\overline{\langle\langle v'^2\rangle\rangle}/\overline{\langle u'^2\rangle}$ at different Re_λ deviate more significantly from each other. This is explained by considering the fact that the heavier particles interact more with the large scale flow structures. We also found that the characteristics time $\tau_T = c\langle u'^2\rangle/\varepsilon$ (c is a constant), which appears in the Hinze–Tchen relation [41] is only appropriate for scaling of $\overline{\langle\langle v'^2\rangle\rangle}/\overline{\langle u'^2\rangle}$ when the flow Reynolds number is sufficiently large. Note that the proper time for scaling of the other particle statistics may be different than that observed for $\overline{\langle\langle v'^2\rangle\rangle}/\overline{\langle u'^2\rangle}$. For example, our results suggest that the particle Reynolds number is properly scaled when the particle response time is normalized by the Kolmogorov time.

The effect of the flow Reynolds number on the particle temperature is similar to that discussed above for the particle velocity. In Fig. 3(a), the variations of $\Delta T = \overline{\langle\langle (T' - T_p')^2\rangle\rangle}/\overline{\langle T'^2\rangle}$ with particle time constant for different flow Reynolds numbers are shown. With increasing the particle time constant, the particle temperature deviate more from the local fluid temperature and ΔT increases. Furthermore, with increasing the flow Reynolds number the effective response time of the particle is increased, accompanied by a corresponding increase in ΔT. Additionally, for the cases considered in Fig. 3, $\alpha = 1$, $Pr = 0.7$ and the structure of the carrier fluid temperature and velocity fields are not very different. Therefore, as shown in Fig. 3(b) the Eulerian eddy turn-over time is also appropriate for scaling of ΔT. Our results also indicate that τ_l is the proper time scale for scaling of $\overline{\langle\langle T_p'^2\rangle\rangle}/\overline{\langle T'^2\rangle}$ (similar to $\overline{\langle\langle v'^2\rangle\rangle}/\overline{\langle u'^2\rangle}$) at different Re_λ.

In the theoretical analysis of particle-laden turbulent flows, the momentum and the heat transfer between the particles and the carrier fluid are usually evaluated via the relations $C_D = 24/Re_p$ and $Nu = 2$. To assess the influence of the non-linearity of the transfer coefficients, the time averaged particle statistics for various particle Reynolds numbers are considered in Table 1. For all cases considered in this table, $\overline{Re_\lambda} = 41.9$, $Pr = 0.7$ and $\alpha = 1$. The particle Reynolds number is varied by changing the particle density while the particle response time is kept constant ($\tau_p = 6$) for all cases. Additional

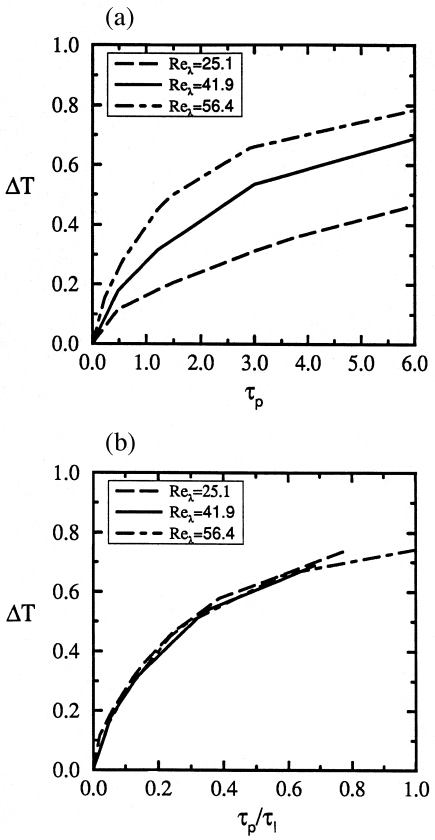

Fig. 3. The variations of $\Delta T = \overline{\langle\langle (T' - T'_p)^2 \rangle\rangle}/\overline{\langle T'^2 \rangle}$ with (a) τ_p; (b) τ_p/τ_l. For all cases $\alpha = 1$ and $Pr = 0.7$.

results are also provided by conducting DNS with $C_D = 24/Re_p$ and $Nu = 2$. The results in Table 1 indicate that the magnitude of $\langle\langle v'^2 \rangle\rangle/\langle u'^2 \rangle$ is increased by 10.4% when $\langle\langle Re_p \rangle\rangle$ increases from 0 to 1.9. The corresponding increase in the magnitude of $\overline{\langle\langle T'^2_p \rangle\rangle}/\overline{\langle T'^2 \rangle}$ is 16.4%. It is also shown that the difference between the particle temperature and the local fluid temperature decreases as the particle Reynolds number increases. The non-linearity of the drag and heat transfer coefficients result in higher values for these coefficients; therefore, the rate of heat transfer between a particle and its surrounding fluid increases, accompanied by an increase in their temperature correlation. Based on the results shown in Table 1, it is concluded that the non-linearity of the transfer coefficients have small effects on the particle statistics when the particle Reynolds number is less than unity.

By relating the Lagrangian equations of particle velocity and temperature, Yarin and Hetsroni [28] obtain:

$$\frac{\langle\langle T'^2_p \rangle\rangle^{1/2}}{\langle T'^2 \rangle^{1/2}} = 1 - \left(1 - \frac{\langle\langle v'^2 \rangle\rangle^{1/2}}{\langle u' \rangle^{1/2}}\right)^{\frac{Nu}{3\alpha Pr}}. \tag{13}$$

In deriving equation (13), it is assumed that the interactions between the particles and the fluid are solely due to the drag force and thermal convection. These interactions are expressed by the relations $C_D = 24/Re_p$ and $Nu = 2$. To assess the validity of equation (13), the ratio of the particle to fluid temperature intensities based on equation (13) ($(TR)_{theory}$) and those via DNS data ($(TR)_{DNS}$) are compared in Table 1 and Fig. 4. The magnitude of Nu in equation (13) is evaluated from equation (10) based on the average value of particle Reynolds

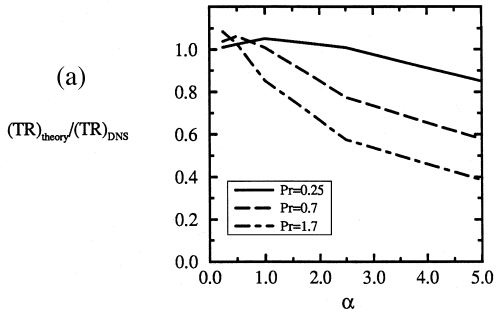

Fig. 4. The variation of the ratio of the model to DNS values of $\langle\langle T'^2_p \rangle\rangle^{1/2}/\langle T'^2 \rangle^{1/2}$ with α. For all cases $Re_\lambda = 41.9$ and $\tau_p = 6$.

Table 1
The variations of the particle statistics with the particle density

ρ_p	C_D	Nu	$\overline{\langle\langle Re_p \rangle\rangle}$	$\overline{\langle\langle v'^2 \rangle\rangle}/\overline{\langle u'^2 \rangle}$	$\overline{\langle\langle T'^2_p \rangle\rangle}/\overline{\langle T'^2 \rangle}$	$\overline{\langle\langle (T' - T'_p)^2 \rangle\rangle}/\overline{\langle T'^2 \rangle}$	$(TR)_{theory}/(TR)_{DNS}$
250	Equation (8)	Equation (10)	1.90	0.566	0.536	0.685	1.113
500	Equation (8)	Equation (10)	1.37	0.556	0.525	0.694	1.098
1000	Equation (8)	Equation (10)	0.97	0.553	0.509	0.704	1.082
4000	Equation (8)	Equation (10)	0.50	0.533	0.497	0.718	1.063
16 000	Equation (8)	Equation (10)	0.25	0.523	0.480	0.727	1.046
1000	$24/Re_p$	2	0.0	0.507	0.448	0.752	0.997
1000	Equation (8)	2	0.97	0.546	0.448	0.749	1.037
1000	$24/Re_p$	Equation (10)	0.97	0.507	0.513	0.706	1.050

number. The results in Table 1 suggest that by increasing $\langle\langle Re_p\rangle\rangle$, the magnitude of $(TR)_{theory}$ exceeds more significantly from that of the $(TR)_{DNS}$. This implies that the predictive capability of equation (13) reduces as particle Reynolds number increases, which is expected due to non-linearity of the transfer coefficients. The difference between DNS and theoretical results is minimum (about 0.3%) when the particle drag and heat transfer coefficients in DNS are evaluated via linear relations. Our results also indicate that the ratio $(TR)_{theory}/(TR)_{DNS}$ does not vary noticeably as the magnitudes of τ_p and Re_p vary. However, this ratio varies significantly with Pr and α. This is observed in Fig. 4, where it is shown that for small values of αPr (<1), equation (13) predicts the DNS results with reasonable accuracy. For large values of αPr, the difference between the DNS and the model values is significant. Also, for large values of αPr, our results indicate that $(TR)_{theory}/(TR)_{DNS}$ increases slightly when τ_p/τ_k (or Re_p) increases. This suggests that the non-linearity of the transfer coefficients is not responsible for the significant difference between the theoretical and numerical results at high αPr values.

In Fig. 5, the temporal evolution of the auto-correlation coefficients of the particle velocity (R_v^p), and temperature (R_T^p) for different particle response times are shown. The time t_D is the time normalized by the Eulerian eddy turn-over time. The coefficients R_v^p and R_T^p represent the memory effects for the particle velocity and temperature, respectively and are calculated when particles reach a stationary state. These coefficients are used to obtain the momentum and the thermal diffusion coefficients (see below) and are defined as:

$$R_v^p = \frac{1}{3}\sum_{m=1}^{3} \frac{\langle\langle v'_m(t_0)v'_m(t_0+\tau)\rangle\rangle}{[\langle\langle v'^2_m(t_0)\rangle\rangle\langle\langle v'^2_m(t_0+\tau)\rangle\rangle]^{1/2}}, \quad (14)$$

$$R_T^p = \frac{\langle\langle T'_p(t_0)T'_p(t_0+\tau)\rangle\rangle}{[\langle\langle T'^2_p(t_0)\rangle\rangle\langle\langle T'^2_p(t_0+\tau)\rangle\rangle]^{1/2}}, \quad (15)$$

where the auto-correlation coefficient of the particle velocity is defined as average of directional coefficients, and t_0 is the starting time for the calculation of the Lagrangian statistics. In statistically stationary flows, t_0 is arbitrary and $\langle\langle v'^2_m(t_0+\tau)\rangle\rangle = \langle\langle v'^2_m(t_0)\rangle\rangle$. Consistent with previous observations [24, 18, 22], it is shown in Fig. 5(a) that the auto-correlation coefficient of the particle velocity increases as the particle response time (inertia) increases. The memory of the particle to its previous velocity increases as the particle inertia increases, thus increasing the correlation coefficient over that for fluid particles. A monotonic increase with τ_p is observed for R_v^p. The Lagrangian auto-correlation coefficient of particle temperature, in addition to τ_p, is dependent on the magnitudes of Pr and α. For small values of Pr (~ 0.25), the rate of heat transfer between the particles and the fluid is significant and particles quickly adjust to the surrounding fluid temperature. Consequently, the auto-correlation coefficient of the particle temperature is not significantly dependent on the magnitude of τ_p (Fig. 5(b)). For higher Prandtl numbers (~ 1.7), the response of particles to the variations in local fluid temperature is slow and the effect of τ_p on R_T^p could be important. It is shown in Fig. 5(c), that for particles with response times close to or smaller than the Kolmogorov time scale, the effect of particle inertia on R_T^p is not significant even when $Pr = 1.7$. As the particle time constant exceeds the Kolmogorov time scale, R_T^p is noticeably increased with τ_p.

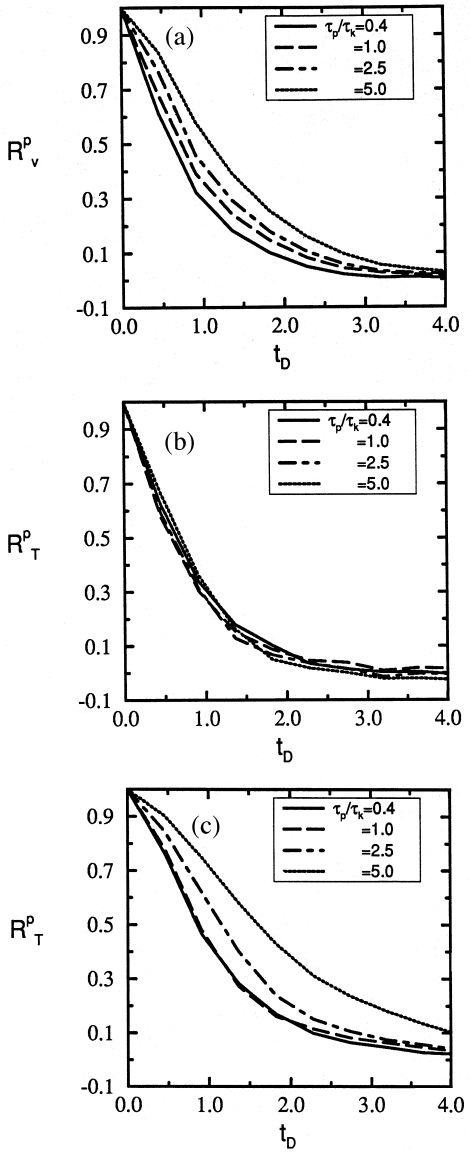

Fig. 5. Temporal variation of the auto-correlation coefficient of the particle velocity and temperature. (a) R_v^p; (b) R_T^p ($Pr = 0.25$); (c) R_T^p ($Pr = 1.7$). For all cases $Re_\lambda = 41.9$ and $\alpha = 1$.

Unlike R_v^p, a monotonic increase with τ_p is not observed for R_T^p. The results shown in Fig. 5(b) and (c) also suggest that the effect of Pr on R_T^p is dependent on the particle response time. We have found that for $\tau_p > \tau_k$ the instantaneous values of R_T^p increase with Pr. As equation (6) implies, the rate of heat transfer between the phases depends on the temperature difference between the particle and the surrounding fluid element. This temperature difference is relatively lower when the particles are light. Consequently, the rate of heat transfer is lower for light particles and R_T^p is less affected by the magnitudes of τ_p and Pr.

The effect of α on R_T^p is shown in Fig. 6, where the temporal evolution of R_T^p for $\alpha = 0.25$ and 5.0 are considered. For $\alpha < 1$, the particles rapidly respond to the surrounding fluid temperature. In this case, as shown in Fig. 6(a), the effects of Pr (also τ_p) on R_T^p are relatively small. For large values of α, particles keep their thermal identity as they are less sensitive to the variations of the carrier fluid temperature. For this case, the auto-correlation coefficient of the particle temperature is considerably more sensitive to the magnitudes of Pr and τ_p (Fig. 6(b)).

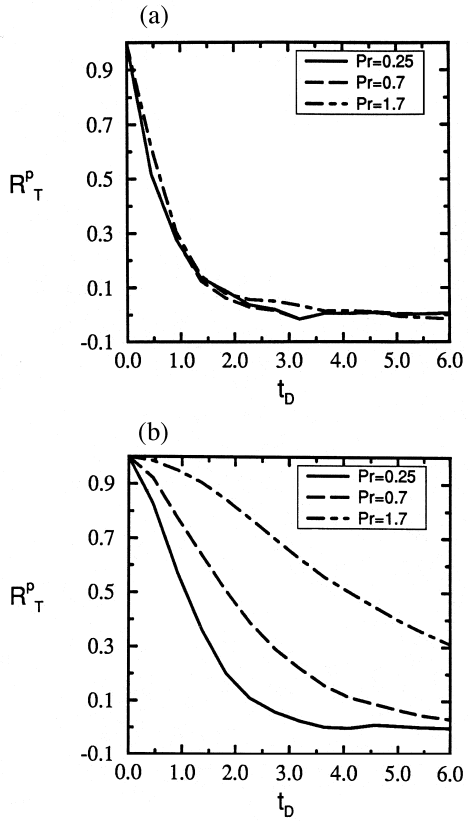

Fig. 6. Temporal variation of the auto-correlation coefficient of the particle temperature. (a) $\alpha = 0.25$; (b) $\alpha = 5$. For all cases $Re_\lambda = 41.9$ and $\tau_p = 3$.

Taylor [7] formulated the diffusive nature of turbulence by relating the coefficient of fluid particle diffusion (D_u^f) to the Lagrangian auto-correlation coefficient of the fluid particle velocity (R_u^f). For large diffusion times, D_u^f is expressed by [44]:

$$D_u^f = \langle u'^2 \rangle \int_0^\infty R_u^f(\tau)\, d\tau. \tag{16}$$

The value of D_u^f as given by equation (16) would also be valid for the transport coefficient of a scalar quantity such as temperature if there were no exchange of this quantity with the surrounding fluid along the trajectory of the fluid particle. However, since the fluid particle consists of very large number of molecules, there is at least a molecular transport between the fluid particle with its surrounding. Therefore, the diffusion coefficient of fluid particle temperature (D_T^f) is expected to be different from D_u^f. Hinze [44] proposes:

$$D_T^f = \langle u'^2 \rangle \int_0^\infty f(\Lambda, \tau) R_u^f(\tau)\, d\tau \tag{17}$$

where Λ is an exchange coefficient and $f(\Lambda, \tau)$ accounts for the effect of the exchange along the path of the fluid particle. The function 'f' is, in general, a complex function of Λ and τ. An exponential model of $f(\Lambda, \tau) = \exp(-\Lambda\tau)$ has been suggested [44].

The magnitude of D_u^f and D_T^f evaluated from equations (16) and (17) represent the long time values of the fluid particle velocity and temperature diffusivity coefficients. For heavy particles, one can similarly define the coefficient of particle momentum diffusion (D_v^p) in terms of the Lagrangian auto-correlation coefficient of particle velocity [12]:

$$D_v^p = \langle v'^2 \rangle \int_0^\infty R_v^p(\tau)\, d\tau. \tag{18}$$

The difference between the fluid velocity and temperature diffusivity coefficients is expressed via the function f. Similarly, we introduce the function f^p that accounts for the exchange of particle heat with the surrounding fluid along the particle path. With this, the particle temperature diffusion coefficient, D_T^p, is calculated as:

$$D_T^p = \langle v'^2 \rangle \int_0^\infty R_T^p(\tau) R_v^p(\tau)\, d\tau \tag{19}$$

where it is assumed that $f^p = R_T^p$. When the heat transfer between particles and the fluid is negligible (e.g., $\alpha Pr \gg 1$), $R_T^p \approx 1$ and as equations (18) and (19) suggest, the long time diffusion of particle temperature is the same as that of the particle velocity ($D_T^p = D_v^p$).

In Fig. 7, the variation of D_T^p/D_v^p with α and τ_p/τ_k for different Pr values are shown. With increasing α and/or Pr, as suggested by Fig. 6 and equation (19), D_T^p increases

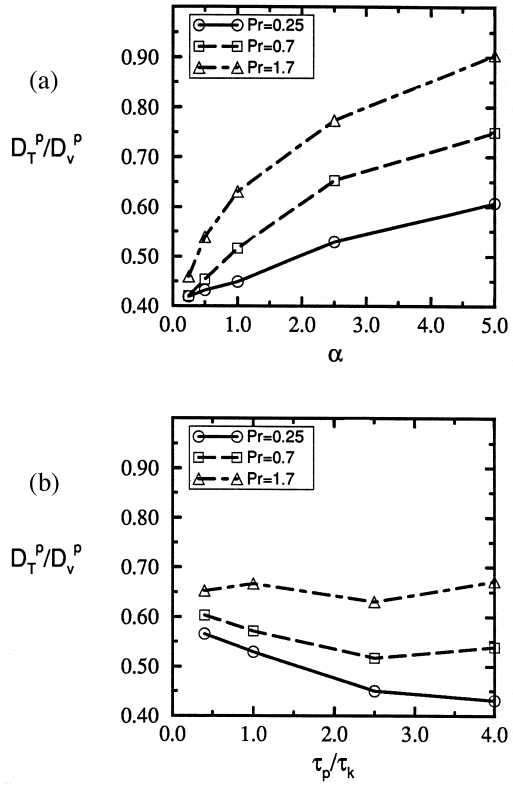

Fig. 7. The variation of D_T^p/D_v^p with (a) α ($\tau_p = 3$); (b) τ_p/τ_k ($\alpha = 1$). For all cases $Re_\lambda = 41.9$.

and becomes closer to D_v^p. This is shown in Fig. 7(a). It is also shown in this figure that D_T^p varies more significantly with α and Pr as the magnitude of αPr increases. The ratio D_T^p/D_v^p is almost independent of α and Pr when the rate of heat transfer is high. The effect of particle inertia on D_T^p/D_v^p is shown in Fig. 7(b). For $Pr = 0.25$, the ratio D_T^p/D_v^p decreases as τ_p/τ_k increases. However, as the magnitude of Pr increases, the effect of τ_p on D_T^p/D_v^p is decreased. With decreasing the size of the particles, the effect of Pr (and α) on D_T^p is decreased. This is understandable since the rate of heat transfer and therefore R_T^p is less sensitive to the magnitude of Pr as the size of the particle decreases (Fig. 5).

3.2. Two-way coupling

Two-way coupling effects are discussed in this subsection. An important parameter in this study is ϕ_m which is varied by changing the number of particles while keeping τ_p constant. As pointed out by Squires and Eaton [25], the particles act as an additional source of dissipation of turbulent kinetic energy. As a result, in stationary turbulence the turbulent kinetic energy decreases as the mass loading ratio increases. The average dissipation rate of the turbulent kinetic energy also decreases as ϕ_m increases. This is observed in Fig. 8(a), where it is shown that by adding more particles to a stationary flow, ε decreases more and after a transient time approaches a stationary value. Initially, the particles are distributed uniformly throughout the domain and have the same velocity as that of the surrounding fluid elements. Therefore, there is a transient time during which both particles and carrier fluid adjust to their new conditions. This transient time was found to be about two to three eddy

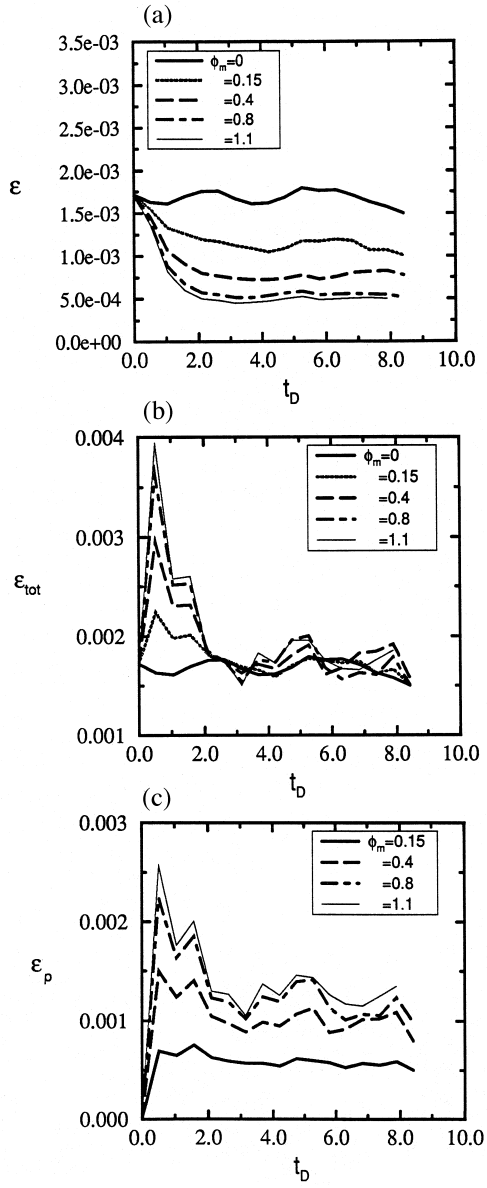

Fig. 8. Temporal variations of the average dissipation rate of energy, (a) ε; (b) ε_{tot}; (c) ε_p. For all cases $\tau_p = 3.6$.

turn-over times, close to the values reported by Squires and Eaton [22]. After this transient time, the balance of energy requires that the energy input by the forcing be the same as the total rate of dissipation of the turbulent kinetic energy (ε_{tot}) by the fluid and particles. As shown in Fig. 8(b), the long time values of ε_{tot} remain fairly constant and independent of the magnitude of ϕ_m. Therefore, the energy added by forcing function to the mixture also remains fairly constant and unaffected by the particles. This indicates that the results obtained here are not contaminated by forcing. The initial increase in ε_{tot} values with ϕ_m is required to decrease the turbulence energy to its lower stationary level. The decrease of ε with the increase of mass loading can be explained by considering the evolution of the average rate of 'dissipation' of energy by the particle drag force,

$$\varepsilon_p = \left\langle \sum \left\{ \frac{C_D Re_p m_p}{24\tau_p}(u_i^* - v_i)u_i^* \right\} \right\rangle. \quad (20)$$

It is to be noted that ε_p may have both positive and negative signs. Therefore this term may remove or add energy to the turbulent kinetic energy, although it refers to the 'dissipation' term here. For the cases considered in this study, ε_p always removes energy from the turbulent kinetic energy.

Figure 8(c) shows that the values of ε_p increase as the mass loading ratio (or the number of particles) increases. This observation together with the previous observation that the long time values of $\varepsilon_{tot} = \varepsilon_p + \varepsilon$ are nearly independent of the mass loading, explains the decrease of ε with the increase of mass loading. Our results (not shown) also indicate that the 'dissipation' of energy by each individual particle (ε_p/N_p) decreases as mass loading ratio increases. The reason is that with increasing the mass loading, the velocity vector of the surrounding fluid aligns better with the direction of the particle trajectory and also the magnitudes of velocities are smaller. Consequently, the particle drag force and the particle Reynolds number are lower for higher mass loadings. Since by increasing ϕ_m, the dissipation of energy by each individual particle decreases, ε_p and ε should not vary linearly with ϕ_m. This is observed in Fig. 8(c), where it is shown that the rate of increase of ε_p with ϕ_m decreases as the magnitude of ϕ_m increases.

The modulation of the flow by the particles may also depend on the particles' response time, as particles with different inertia correlate differently with different scales of the flow. For the range of parameters considered, the magnitude of τ_p does not have a significant impact on the evolution of the turbulence energy. This is observed in Fig. 9(a), where it is shown that for constant mass loading ratio, the turbulent energy does not vary appreciably as τ_p/τ_k varies. For small particles, the main interaction between the particles and the fluid occurs at small scales. Therefore, the turbulence energy is not significantly dependent on the size of particles. However, the dissipation rate of the turbulence kinetic energy noticeably decreases as the size of particles increase (Fig. 9(b)). This is true since for stationary turbulence, the total energy dissipated by the fluid and particles is constant, equal to the forcing energy, and independent of the size of particles. Therefore, with increasing τ_p, ε has to decrease because the drag force and ε_p increase.

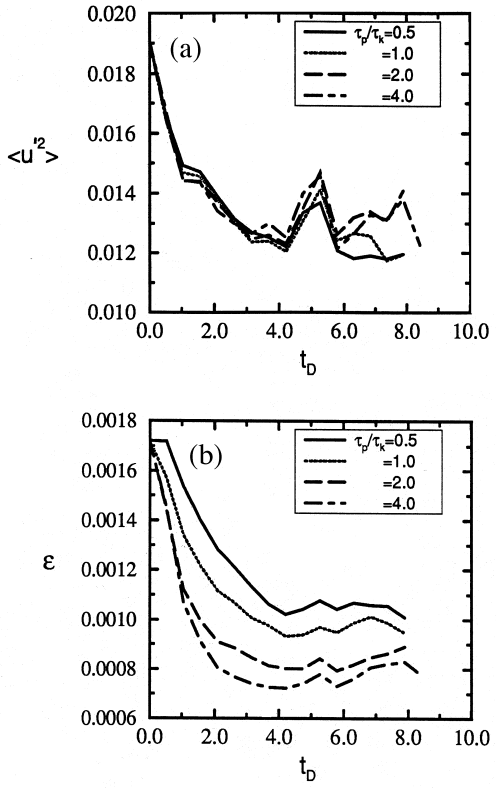

Fig. 9. Temporal variations of the carrier fluid (a) velocity variance (energy); (b) dissipation rate of energy for different particle response time and for $\phi_m = 0.4$.

The effects of particles on different scales of the fluid velocity and temperature are considered in Fig. 10, where the three-dimensional velocity and temperature spectral density functions (E, E_T) for $\phi_m = 0$ and 0.4 are shown. Consistent with the results of Squires and Eaton [25], it is observed that the high wavenumber values of the fluid velocity spectrum are significantly increased by the particles. The effect of particles on the fluid velocity dissipation spectra is similar. The three-dimensional fluid temperature spectrum also exhibits similar behavior to that of the velocity, as the results in Fig. 10 indicate that the high wavenumber spectral values of the fluid temperature are increased by the particles. This suggests that the thermal and momentum interactions of the particles and the carrier fluid at small scales are qualitatively similar. The modification of the fluid velocity and tem-

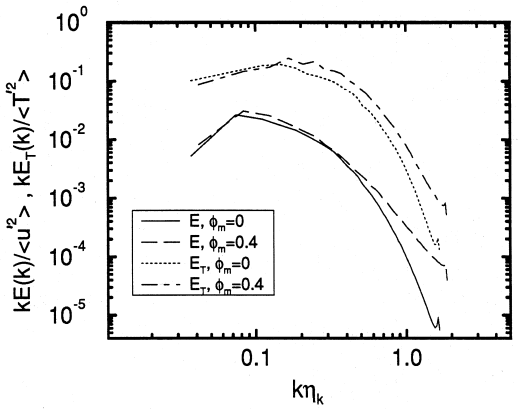

Fig. 10. The spectral densities of the fluid velocity and temperature for $\phi_m = 0$ and 0.4 and $\tau_p/\tau_k = 1$.

perature fields also results in the variation of the particle temperature statistics due to two-way coupling effects. An example is the auto-correlation coefficient of the particle temperature, which is shown in Fig. 11 to increase with ϕ_m. Additionally, Fig. 11 illustrates that for two cases with the same mass loading, the values of R_T^p decrease significantly when the effect of the particles on the fluid velocity field is eliminated ($S_{Mi} = 0$). However, the values of R_T^p in the case that $\phi_m = 0.8$ and $S_{Mi} = 0$ are still higher than those in the case with $\phi_m = 0$. This suggests that R_T^p increases with ϕ_m for two reasons. First, the particles correlate more with the path of the fluid elements due to momentum coupling. Second, the deviation between the particle and fluid temperatures decreases due to thermal coupling.

Time averaged values of some other statistical quantities which are affected by two-way coupling are listed

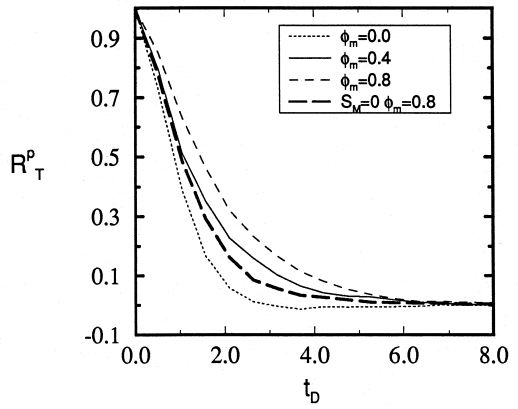

Fig. 11. Temporal variation of the auto-correlation coefficient of the particle temperature for $\tau_p = 3.6$, $\alpha = 1$ and $Pr = 0.7$.

in Table 2. The first four rows in this table represent the results for mass loading ratios from 0–1.1. The last row corresponds to the case with $\phi_m = 0.8$, $S_{Mi} = 0$. Expectedly, with increasing the mass loading ratio the magnitude of Re_λ decreases. Consequently, the time scales associated with fluid velocity field increase and the effective response time of the particles decrease. Additionally, with an increase in the mass loading, the coupling between velocity and temperature of the particles with those of the surrounding fluid element increases. As a result, $\langle\langle Re_p\rangle\rangle$, $\langle T'^2\rangle$, $\langle\langle T_p'^2\rangle\rangle/\langle T'^2\rangle$, and ε_T all decrease. The results in Table 2 also demonstrate that the magnitudes of $\langle\langle T_p'^2\rangle\rangle/\langle T'^2\rangle$ and $\varepsilon_T/(\varepsilon_T)_{\phi=0}$ for the case with $\phi_m = 0.8$, $S_{Mi} = 0$ are lower than those for the case with $\phi_m = 0.8$, $S_{Mi} \neq 0$. These results are in accord with those shown in Fig. 11, and suggest that the effects of fluid-particle thermal and momentum coupling are both important.

Also listed in Table 2 is the correlation coefficient between the temperature and its dissipation rate,

$$\xi_T = \frac{\langle T'^2\varepsilon_T\rangle}{\langle T'^2\rangle\langle\varepsilon_T\rangle} - 1. \tag{21}$$

The correlation between temperature and its dissipation reflects the correlation between large and small scale temperature fluctuations [45, 46]. This correlation is also an indicator of the 'non-Gaussianity' of the probability density function (PDF) of the temperature. The results in Table 2 show that with increasing the mass loading, the correlation between temperature and its dissipation increases and the PDF of temperature departs more from a Gaussian distribution. Another indicator of the non-Gaussianity of the temperature PDF is the deviation of the temperature kurtosis from the Gaussian value of 3. The kurtosis was found to increase from 2.98 to 3.61 when ϕ_m increases from 0 to 1.1.

4. Summary and conclusion

Direct numerical simulations (DNS) of homogeneous particle-laden turbulent flows are conducted to investigate the thermal transport and the particle and fluid temperature behavior in dilute two-phase flows. Both one-way and two-way coupling between the particles and the carrier fluid are considered. The important parameters that characterize the temperature statistics are the particle response time (τ_p), the ratio of the specific heats (α), the Prandtl number (Pr), the Reynolds number (Re_λ), and the mass loading ratio (ϕ_m). The influences of these parameters on both the fluid and the particle temperature statistics are examined.

In a qualitative agreement with theoretical observations [28], the DNS results indicate that the stationary value of the particle temperature intensity is a decreasing

Table 2
The variations of the particle statistics with the mass loading ratio

ϕ_m	$\overline{Re_\lambda}$	τ_p/τ_k	$\overline{\langle\langle Re_p\rangle\rangle}$	$\overline{\langle\langle T_p'^2\rangle\rangle}/\overline{\langle T'^2\rangle}$	$\overline{\varepsilon_T}/\overline{(\varepsilon_T)_{\phi=0}}$	$\overline{\xi_T}$
0.0	49.1	3.81	0.808	0.613	1.0	−0.039
0.4	46.8	2.60	0.531	0.580	0.543	0.103
0.8	41.8	2.27	0.424	0.501	0.455	0.243
1.1	37.3	2.17	0.371	0.446	0.439	0.319
0.8	49.1	3.81	0.808	0.485	0.348	0.238

function of τ_p, α and Pr. The particle temperature intensity is also a decreasing function of Re_λ. However, the particle velocity and temperature quantities which are mainly dependent on the large scales of the flow can be well scaled with Re_λ, if the particle response time is normalized by the Eulerian eddy turn-over time. If the response time of the particles is less than the Kolmogorov time or the variable is mainly small scale dependent, the Kolomogorov time is appropriate for scaling.

The auto-correlation coefficient of the particle temperature, R_T^p exhibits different behavior than that of the particle velocity, R_v^p. Unlike R_v^p, a monotonic increase with τ_p is not observed for R_T^p. For small values of αPr and/or τ_p, R_T^p is not significantly dependent on the magnitude of τ_p, Pr and α. For higher values of αPr and τ_p, R_T^p increase noticeably with τ_p, Pr and α. The results for R_v^p and R_T^p are used to evaluate the long time values of the particle velocity and temperature diffusion coefficients (D_v^p and D_T^p, respectively). The ratio of D_T^p/D_v^p is less than unity but tends toward unity when the magnitudes of α and/or Pr increase. The rate at which D_T^p/D_v^p increases is higher for higher values of αPr.

The fluid and particle statistics are also affected by the two-way coupling effects. By increasing the mass loading ratio the coupling between the velocity of the particle and that of the surrounding fluid increases, and both the particle and the flow Reynolds numbers decrease. Also, the ratio of particle to fluid temperature intensities and the dissipation of fluid temperature fluctuations (ε_T) decrease as the mass loading increases. Additionally, by increasing the mass loading ratio, the coupling between the temperature and its dissipation rate as well as the deviation of the fluid temperature PDF from Gaussianity increases. The modification of the fluid and particle temperature statistics is not solely due to modification of the fluid velocity field by the particles; thermal coupling is also important.

Our results reveal several important physical features of thermal transport in two-phase turbulent flows and indicate that the thermal interaction between phases is important and cannot be overlooked in modeling of these flows. The next challenging step would be the DNS study of thermal transport in non-reacting and reacting inhomogeneous turbulent flows.

References

[1] G.M. Faeth, Mixing, transport and combustion in sprays, Prog. Energy Combust. Sci. 13 (1987) 293–345.
[2] J.K. Eaton, J.R. Fessler, Preferential concentration of particles by turbulence, Int. J. Multiphase Flow 20 (1994) 169–209.
[3] J.B. McLaughlin, Numerical computation of particles-turbulence interaction, Int. J. Multiphase Flow 20 (1994) 211–232.
[4] C.T. Crowe, T.R. Troutt, J.N. Chung, Numerical models for two-phase turbulent flows, Ann. Rev. Fluid Mech. 28 (1996) 11–43.
[5] J.S. Shirolkar, C.F.M. Coimbra, M.Q. McQuay, Fundamental aspects of modeling turbulent particle dispersion in dilute flows, Prog. Energy Combust. Sci. 22 (5) (1996) 363–399.
[6] E.E. Michaelides, Review—the transient equation of motion for particles, bubbles, and droplets, Journal of Fluids Engineering 119 (1997) 233–247.
[7] G.I. Taylor, Diffusion by continuous movements, Proc. Lond. Math. Soc. (2), 20 (1921) 196–211.
[8] A.S. Monin, A.M. Yaglom, Statistical fluid mechanics, Vol. 2, MIT Press, Cambridge, MA, 1975.
[9] K. Kontomaris, T.J. Hanratty, Effect of molecular diffusivity on turbulent diffusion in isotropic turbulence, Int. J. Heat Mass Transfer 36 (5) (1993) 1403–1412.
[10] M.S. Borgas, B.L. Sawford, A family of stochastic models for two-particle dispersion in isotropic homogeneous stationary turbulence, J. Fluid Mech. 279 (1994) 69–99.
[11] M.I. Yudine, Physical considerations on heavy-particle diffusion, Adv. Geophys. 6 (1959) 185–191.
[12] G.T. Csanady, Turbulent diffusion of heavy particles in the atmosphere, J. Atmos. Sci. 20 (1963) 201–208.
[13] M.W. Reeks, On the dispersion of small particles suspended in an isotropic turbulent fluid, J. Fluid Mech. 83 (1977) 529–546.
[14] A. Nir, L.M. Pismen, The effect of steady drift on the dispersion of a particle in turbulent fluid, J. Fluid Mech. 94 (1979) 369–381.
[15] R. Mei, R.J. Adrian, T.J. Hanratty, Particle dispersion in isotropic turbulence under Stokes drag and Basset force with gravitational settling, J. Fluid Mech. 225 (1991) 481–495.
[16] K.K. Kuo, Principles of combustion, John Wiley and Sons, New York, NY, 1986.
[17] W.H. Snyder, J.L. Lumley, Some measurements of particle

velocity autocorrelation functions in a turbulent flow, J. Fluid Mech. 48 (1971) 41–47.
[18] M.R. Wells, D.E. Stock, The effects of crossing trajectories on the dispersion of particles in a turbulent flow, J. Fluid Mech. 136 (1983) 31–62.
[19] S. Schreck, S.J. Kleis, Modification of grid-generated turbulence by solid particles, J. Fluid Mech. 249 (1993) 665–688.
[20] P. Givi, Model free simulations of turbulent reactive flows, Prog. Energy Combust. Sci. 15 (1989) 1–107.
[21] J.J. Riley, G.S. Patterson, diffusion experiments with numerically integrated isotropic turbulence, Phys. Fluids 17 (1974) 292–297.
[22] K.D. Squires, J.K. Eaton, Measurements of particle dispersion obtained from direct numerical simulations of isotropic turbulence, J. Fluid Mech. 226 (1991) 1–35.
[23] S. Elghobashi, G.C. Truesdell, Direct simulation of particle dispersion in a decaying isotropic turbulence, J. Fluid Mech. 242 (1992) 655–700.
[24] L.M. Pismen, A. Nir, On the motion of suspended particles in stationary homogeneous turbulence, J. Fluid Mech. 84 (1978) 193–206.
[25] K.D. Squires, J.K. Eaton, Particle response and turbulence modification in isotropic turbulence, Phys. Fluids 2 (7) (1990) 1191–1203.
[26] S.L. Soo, (Ed.), Multiphase fluid dynamics, science press/grower technical, Beijing/Sydney, 1990.
[27] A.A. Shraiber, L.B. Gavin, V.A. Naumov, V.P. Yatsenko, Turbulent flows in gas suspensions, Hemisphere, New York, NY, 1990.
[28] L.P. Yarin, G. Hetsroni, Turbulence intensity in dilute two-phase flows. II Temperature fluctuations in particle-laden dilute flows, Int. J. Multiphase Flow, 20 (1) (1994) 17–25.
[29] T.W. Park, S.K. Aggarwal, V.R. Katta, Gravity effects on the dynamics of evaporating droplets in a heated jet, J. Propulsion and Power 11 (3) (1995) 519–528.
[30] Z. Warhaft, J.L. Lumley, An experimental study of the decay of temperature fluctuations in grid-generated turbulence, J. Fluid Mech. 88 (1978) 659.
[31] S. Tavoularis, S. Corrsin, Experiments in nearly homogeneous turbulent shear flow with a uniform mean temperature gradient. Part 1, J. Fluid Mech. 104 (1981) 311–347.
[32] R.M. Kerr, High-order derivative correlations and the alignment of small-scale structures in isotropic numerical turbulence, J. Fluid Mech. 153 (1985) 31–58.
[33] W.E. Ranz, W.R. Marshall, Evaporation from drops, Chem. Engineering Prog. 48 (1952) 141–173.
[34] G.M. Faeth, Evaporation and combustion of sprays, Prog. Energy Combust. Sci. 9 (1983) 1–76.
[35] A. Berlemont, M.S. Grancher, G. Gouesbet, On the Lagrangian simulation of turbulence influence on droplet evaporation, Int. J. Heat Mass Transfer 34 (11) (1991) 2805–2812.
[36] C.T. Crowe, M.P. Sharma, D.E. Stock, The particle-source-in cell (PSI-cell) model for gas–droplet flows, J. Fluids Engineering (1977) 325–332.
[37] G.B. Wallis, One-dimensional two-phase flow, McGraw-Hill Book Company, New York, NY, 1969.
[38] P. Givi, C.K. Madnia, Spectral methods in combustions, in: T.J. Chung (Ed.), Numerical Modeling in Combustion, Taylor & Francis, New York, NY, 1993, pp. 409–452.
[39] F.A. Jaberi, R.S. Miller, C.K. Madnia, P. Givi, Non-Gaussian scalar statistics in homogeneous turbulence, J. Fluid Mech. 313 (1996) 241–282.
[40] V. Eswaran, S.B. Pope, Direct numerical simulations of the turbulent mixing of a passive scalar, Phys. Fluids 31 (3) (1988) 506–520.
[41] L.X. Zhou, (Ed.), Theory and Numerical Modeling of Turbulent Gas-Particle Flows and Combustion, CRC Press, Florida, U.S.A., 1993.
[42] C.T. Crowe, J.N. Chung, T.R. Troutt, Particle mixing in free shear flows, Prog. Energy Combust. Sci. 14 (1988) 171–194.
[43] S.K. Aggarwal, Relationship between Stokes number and intrinsic frequencies in particle-laden flows, AIAA J. 32 (6) (1994) 1322–1325.
[44] J.O. Hinze, Turbulence, McGraw-Hill Book Company, New York, NY, 1975.
[45] F. Anselmet, H. Djeridi, L. Fulachier, Joint statistics of a passive scalar and its dissipation in turbulent flows, J. Fluid Mech. 280 (1994) 173–197.
[46] J. Mi, R.A. Antonia, F. Anselmet, Joint statistics between temperature and its dissipation rate components in a round jet, Phys. Fluids 7 (7) (1994) 1665–1673.